FEBS Letters 585 (2011) 1821–1827

journal homepage: www.FEBSLetters.org

Arabidopsis actin-depolymerizing factors (ADFs) 1 and 9 display antagonist activities

Stéphane Tholl, Flora Moreau, Céline Hoffmann, Karthik Arumugam, Monika Dieterle, Danièle Moes, Katrin Neumann, André Steinmetz, Clément Thomas *

Centre de Recherche Public-Santé, L-1526 Luxembourg, Luxembourg

ARTICLE INFO

Article history:
Received 14 March 2011
Revised 2 May 2011
Accepted 3 May 2011
Available online 11 May 2011

Edited by Dietmar J. Manstein

Keywords:
Actin
Actin bundling
ADF
Cofilin
Arabidopsis

ABSTRACT

We provide evidence that one of the 11 *Arabidopsis* actin-depolymerizing factors (ADFs), namely ADF9, does not display typical F-actin depolymerizing activity. Instead, ADF9 effectively stabilizes actin filaments in vitro and concomitantly bundles actin filaments with the highest efficiency under acidic conditions. Competition experiments show that ADF9 antagonizes ADF1 activity by reducing its ability to potentiate F-actin depolymerization. Accordingly, ectopic expression of ADF1 and ADF9 in tobacco cells has opposite effects. ADF1 severs actin filaments/bundles and promotes actin cytoskeleton disassembly, whereas ADF9 induces the formation of long bundles. Together these data reveal an additional degree of complexity in the comprehension of the biological functions of the ADF family and illustrate that antagonist activities can be displayed by seemingly equivalent actin-binding proteins.

1. Introduction

The actin-depolymerizing factors (ADFs) and the closely related cofilins in vertebrates and yeast define one of the most highly and widely expressed family of actin-binding proteins which play central roles in the control of actin cytoskeleton dynamics. A substantial body of work has revealed the various activities displayed by ADF/cofilins as well as the numerous signaling pathways controlling these activities [1,2]. In vitro, ADF/cofilins enhance the rate of AF turnover by promoting AF severing and/or facilitating pointed end depolymerization [3–9]. In the presence of high concentrations of ATP-loaded actin monomers, uncapped ends of ADF/cofilin-severed filaments can alternatively be used to increase polymerization. At high ADF/cofilin:actin ratios, ADF/cofilins have also been reported to promote actin nucleation by a yet unclear mechanism [3,5,10,11]. In addition to their functions at the single filament level, ADF/cofilins also likely play central roles in the remodeling of higher order cytoskeletal structures, e.g. by dissociating AF branches mediated by the ARP2/3 complex [12,13].

Animal and plant ADFs are encoded by an ancient gene family. In contrast to vertebrates which typically possess three ADFs/cofilins, plants exhibit particularly large families of ADFs. For instance, *Arabidopsis* expresses 11 functional ADFs which can be classified into four subclasses according to their tissular expression and phylogeny [14,15]. Expression analyses have suggested a model of ADFs co-evolving with the ancient and divergent actin isovariants [15]. Such a model is supported by elegant work showing that the phenotypic changes induced by the ectopic expression of a reproductive class actin in vegetative tissues can be specifically suppressed by co-expression of reproductive profilin and ADF isovariants [16]. Functional specificities among plant ADFs are also suggested by a relatively high degree of protein sequence variation [15]. As an example, *Arabidopsis* ADF1 (subclass I) and ADF9 (subclass III) which are co-expressed in a wide range of tissues [5,9,15,17], only share 53% identity (78% similarity). The biochemical properties of ADF1 have been previously examined in details [5,9,17]. Noticeably, ADF1 enhances AF turnover by increasing the depolymerization rate [5]. Accordingly, the over- and down-expression of *ADF1* in transgenic *Arabidopsis* plants reduces and increases the number of cellular filamentous actin structures, respectively [18]. Although a reduction of the *ADF9* expression level in *Arabidopsis* insertion mutant lines has been shown to induce developmental defects which might be assigned to a dysfunction of the actin cytoskeleton organization and/or dynamics [19], ADF9 actin regulatory activities have not been characterized so far. Here we provide evidence that ADF9 exhibits a surprisingly high ability to stabilize and crosslink AFs. Both in vitro biochemical studies and ectopic expression experiments in tobacco BY2 cells suggest that ADF9 primarily functions as an actin bundling protein whose activity is modulated by pH.

* Corresponding author.
E-mail address: clement.thomas@crp-sante.lu (C. Thomas).

0014-5793/$36.00
doi:10.1016/j.febslet.2011.05.019

2. Materials and methods

2.1. Expression and purification of recombinant proteins

Actin depolymerizing factor 1 (U48938) and ADF9 (NP_195223) coding sequences were PCR-amplified using cDNA prepared from 10 day-old *Arabidopsis* seedlings and cloned into the *Nco*I–*Bam*HI sites of the bacterial expression vector pQE-60 (Qiagen). His6-tagged recombinant proteins were expressed in M15[pREP4] bacteria and purified using a Ni-NTA resin following procedures described by the manufacturer (Qiagen). Purified proteins were dialyzed against a buffer containing 10 mM Tris–Cl, 50 mM NaCl, 1 mM DTT, pH 7.0 using a 10 K molecular weight cutoff dialysis cassette (Pierce) and stored on ice. Prior to an experiment, proteins were pre-clarified at 100 000×*g*, checked for correct mass by SDS–PAGE analysis, and their concentration was determined by Bradford assay (Bio-Rad) using bovine serum albumin as standard. Recombinant WLIM1 (NP_172491) was prepared as previously described in Papuga et al. [27].

2.2. F-Actin depolymerization assays

Rabbit muscle pyrene-labeled actin (4 μM, 30% pyrene-labeled; Cytoskeleton) was polymerized for 1 h 30 min at 20 °C in 50 mM KCl, 2 mM $MgCl_2$, 0.4 mM DTT and 0.5 mM ATP. Depending on the pH tested, the reaction medium was buffered with either MES (7 mM) and PIPES (10 mM), pH 6.0, or PIPES (7 mM) and Tris (10 mM), pH 8.0. Depolymerization was induced by diluting samples to a final actin concentration of 0.4 μM using a buffer containing various amounts of ADF1 and/or ADF9. The decrease in pyrene fluorescence was recorded after dilution over 200 s using a PTI QM-4 QuantaMaster fluorimeter.

2.3. High and low speed cosedimentation assays

Rabbit muscle actin (4 μM, Cytoskeleton) was copolymerized with different amounts of ADF9 or ADF1 for 1 h at 20 °C in 50 mM KCl, 2 mM $MgCl_2$, 0.4 mM DTT and 0.5 mM ATP. Alternatively, AFs were prepolymerized and subsequently incubated 45 min with ADFs. As in F-actin depolymerization assays, the final pH was adjusted to 6.0 or 8.0 using MES (7 mM) and PIPES (10 mM) or PIPES (7 mM) and Tris (10 mM), respectively. Samples were centrifuged at 150 000×*g* (high speed) or 12 000×*g* (low speed) for 30 min at 4 °C and analyzed by SDS–PAGE and Coomassie Brillant Blue R staining (Sigma–Aldrich). In low speed cosedimentation assays, the respective amounts of actin in pellet and supernatant fractions were quantified using ImageJ software (National Institutes of Health). The average percentage of total actin that sediments was calculated from four independent experiments.

2.4. Fluorescence microscopy of actin filaments

Actin (4 μM) was polymerized alone or in the presence of ADF9, ADF1 or WLIM1 and labeled with 0.5 μM Alexa-488-phalloidin (Invitrogen) prior to observation. Alternatively, AFs were labeled with an equimolar amount of Alexa 488-phalloidin and subsequently diluted to 10 nM in fluorescence buffer containing 10 mM imidazole, 50 mM KCl, 1 mM $MgCl_2$, 100 mM DTT, 100 μg/ml glucose oxidase, 15 mg/ml glucose, 20 μg/ml catalase and 0.5% methylcellulose. A sample of 3 μl was applied to a cover slip coated with poly-L-lysine (0.01%). Images were recorded with a Zeiss LSM510 laser scanning confocal microscope using a pinhole set to produce thick (2 μm) optical sections.

In F-actin depolymerization assays (Section 2.2), an aliquot of diluted samples (0.4 μM actin) was labeled with an equimolar amount of Alexa 488-phalloidin immediately after the recording of the last time point (200 s after dilution) and imaged as described above.

2.5. Plasmid constructs for BY2 cell transfection

The plasmids used for tobacco BY2 cell (*Nicotiana tabacum* vc Bright Yellow 2) transfection derive from in-house-constructed plasmids produced by the assembly of plant-specific regulatory regions (35S promoter and nos terminator), the coding sequence of eGFP and the *Nco*I and *Bam*HI restriction sites allowing the subcloning of any coding sequence of interest to produce N-terminally (pNTL2) or C-terminally (pNTL3) GFP-fused proteins, all in a derivative of pBluescript II KS (Stratagene). The coding sequences of the *Arabidopsis* ADF9 and ADF1 genes were introduced in the above described plasmids after PCR amplification using primers containing the appropriate restriction sites and, when necessary, a stop codon.

2.6. BY2 cell transfection

BY2 suspension cells were vacuum-filtrated onto filter paper discs which were laid onto 0.8% agar solid medium. Cell bombardment was performed using gold particles (Sigma–Aldrich) and the PDS-1000/He biolistic particle delivery system from BioRad following manufacturer's instructions. The stopping screen was set at a distance of 11 cm and 1100 psi rupture disks were used. To achieve similar expression levels of the different transgenes, particles were coated with 1 μg of plasmid. In the case of GFP-fused ADF9 encoding plasmids, a low amount of plasmid, i.e., 0.01 μg, was also used to show a dose-dependent effect. Prior to confocal microscopy analyses, bombarded cell samples were kept at 27 °C in the dark for 8 h.

2.7. Live cell confocal microscopy and imaging

Cells expressing GFP and YFP fusion proteins were imaged using a Zeiss LSM510 confocal microscope equipped with a ×40 Plan-NeoFluar oil immersion objective (numerical aperture 1.3). Green Fluorescent Protein and YFP were detected using the 488 nm laser line in combination with a 505–530 nm band-pass emission filter. Rhodamine-phalloidin labeling was performed in PME buffer (50 mM PIPES, 20 mM $MgCl_2$, and 50 mM EGTA). Rhodamine was detected using the 543 nm laser line in combination with a 560–615 nm band-pass emission filter. Confocal images were deconvoluted using Huygens Essential image processing software package (Scientific Volume Imaging) and are shown as projections of neighboring stacks reconstructed using ImageJ software (National Institutes of Health).

2.8. Structure prediction of ADF9

Initial models of ADF9 were built by homology modeling using MODELER9v7 on Unix operating environment [20], which optimally satisfies the spatial restraints derived from the sequence alignment. Data were expressed as Probability Density Functions (PDFs) for comparative protein structure modeling using the crystal structure of ADF1 (PDB: 1F7S) as a template. The primary 3D structure of ADF9 was further improved by molecular dynamics (MD). Equilibration methods were run on a 64 CPU parallel computer using the program CHARMM35 (Chemistry at Harvard Macromolecular Mechanics) force field [21]. The crystallized structure of ADF1 was also refined through energy minimization. Finally, long time MD simulations were run using Langevin dynamics with a time step of 2 fs for both ADF1 and ADF9. This long time MD simulation provided the advantage of iteratively tracking the trajec-

tory of conformational changes in both ADF1 and ADF9. Good accuracy for ADF1 and ADF9 structures was observed with the lowest minimized energy and the least Root Mean Square Deviation (R.M.S.D.).

3. Results and discussion

3.1. ADF9 stabilizes AFs in a concentration dependent manner

One central and presumably biologically relevant property of ADF/cofilins is their ability to accelerate AF disassembly. Another common feature of most plant and animal ADF/cofilins is that they exhibit a pH-sensitive activity, with an enhanced capacity to depolymerize AFs at high pH [5,22–26]. The ability of ADF9 to bind to AFs and to modify the rate of actin depolymerization in physiologically relevant acidic and alkaline conditions was assessed in in vitro assays using ADF1 as a reference.

Fig. 1 shows typical high speed (150 000×*g*) cosedimentation data obtained after incubation of 4 μM pre-polymerized AFs with various amounts of ADF1 or ADF9 (0.5–6 μM) at pH 6.0 or pH 8.0. Both ADF1 and ADF9 bound to AFs in a direct and efficient manner at both pH values. In agreement with previous biochemical studies [5,9], ADF1 promoted partial depolymerization of AFs as indicated by increased amounts of actin in the supernatant fractions (Fig. 1C and D). As expected, the extent of ADF1-induced depolymerization was greater in alkaline than in acidic conditions. In contrast to ADF1, ADF9 did not promote AF depolymerization as indicated by actin sedimentation profiles identical to those of controls (Fig. 1A and B). Although ADF9 interacted with AFs in both pH conditions, this interaction was enhanced in acidic conditions as shown by very low amounts of ADF9 in the supernatant fractions.

To examine the effect of ADF9 binding on AF dynamics, 4 μM pre-polymerized (30%) pyrene-labeled AFs were induced to depolymerize by a 10-fold dilution (0.4 μM actin final) in the presence of increasing concentrations of ADF9 or ADF1 (reference, 8 nM–0.8 μM). Control experiments (no ADF) show the decrease of fluorescence due to AF depolymerization (Fig. 2A–F). Fig. 2A and B show that ADF1 accelerates the decrease of fluorescence in a concentration-dependent manner at both pH 6.0 and 8.0 (Fig. 2A and B). Noticeably, this effect was stronger in basic than in acidic conditions as indicated by sharper curves (compare Fig. 2A and B). In contrast to ADF1, ADF9 effectively reduced the decrease of fluorescence in a concentration-dependent manner (Fig. 2C and D). Although ADF9 was significantly active in the two pH conditions tested, it exhibited a slightly higher efficiency in acidic conditions. For instance, 0.8 μM ADF9 fully stabilized the fluorescent signal only at pH 6.0. The previously reported propensity of ADFs to quench pyrene-actin fluorescence (e.g. Carlier et al., 1997) prompted us to confirm that ADF1 and ADF9 have dissimilar effects on AF depolymerization kinetics. Therefore, 200 s after their dilution, the above samples were stained with Alexa-488-phalloidin, and readily examined by light microscopy (Fig. 2G–L). Controls (no ADF) exhibited substantial amounts of filamentous actin at both pH 6.0 and 8.0 (Fig. 2G and J), indicating that only partial depolymerization had occurred over the time frame of the fluorimetric assay. In contrast, very little or no filamentous actin could be detected in samples containing 0.16 μM of ADF1 (Fig. 2H and K) confirming that ADF1 had accelerated AF disassembly. On the opposite, many filamentous structures were observed in samples containing 0.16 μM of ADF9 (Fig. 2I and L). Consistent with the stabilizing activity suggested for ADF9 by fluorimetric data, these structures appeared more abundant and brighter than the filaments observed in controls (compare Fig. 2I and L to Fig. 2G and J, respectively). This supports that ADF9 is able to stabilize AFs.

Since ADF1 and ADF9 are co-expressed in some tissues [15], and to see if and how ADF9 can affect ADF1 activity and vice versa, competition experiments were conducted using pyrene-labeled actin depolymerization assays. The data obtained using a fixed concentration of ADF1 (1.6 μM) and simultaneously increasing concentrations of ADF9 (0.16–8 μM) indicate that ADF9 counteracts ADF1 in a concentration-dependent manner (Fig. 2E and F). In agreement with the pH preference of each protein, a given concentration of ADF9 more markedly reduced the effects of ADF1 on fluorescence kinetics at pH 6.0 than at pH 8.0. Conversely, experiments conducted with a fixed concentration of ADF9 and increasing concentrations of ADF1 revealed that ADF1 effectively reduces ADF9 activity with the highest efficiency in basic pH conditions (data not shown).

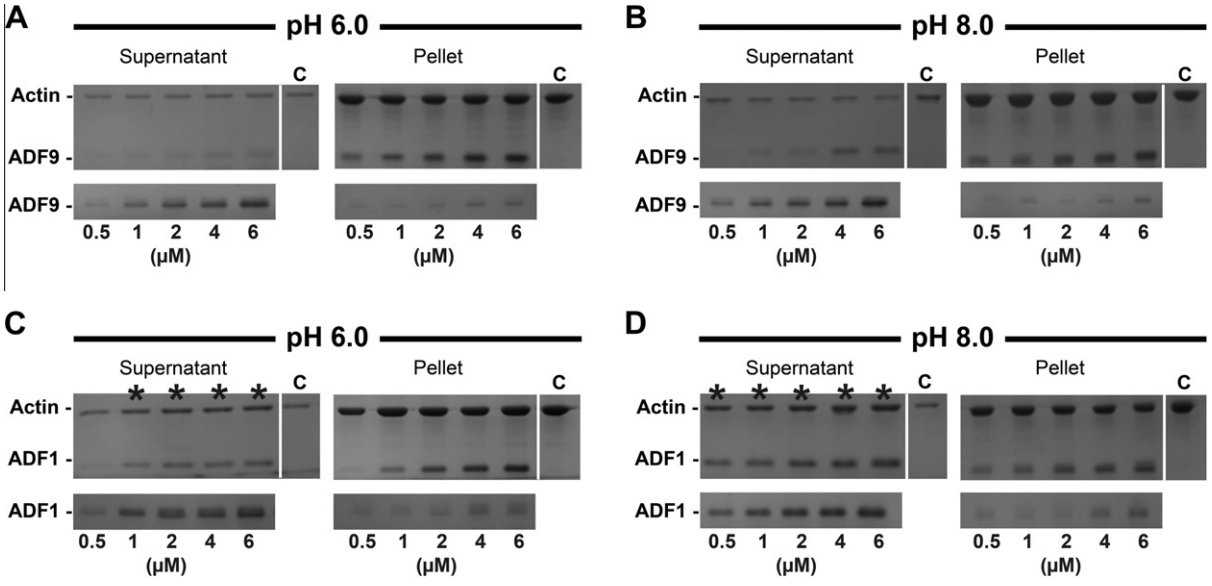

Fig. 1. ADF9 binds to AFs and does not promote actin depolymerization in vitro. Actin filaments (4 μM) were incubated with various amounts of ADF9 (A and B) or ADF1 (C and D) at pH 6.0 (A and C) or 8.0 (B and D) for 45 min and subsequently centrifuged 30 min at 150 000×*g*. Pellet and supernatant fractions were analyzed by SDS–PAGE. The lower gel panels (A–D) show the results of similar experiments conducted in the absence of actin filaments. Note that ADF1 and ADF9 predominantly accumulate in the supernatant fraction. Asterisks indicate the supernatant fractions of samples that contain significantly higher amounts of actin than the control (AFs alone). C: control.

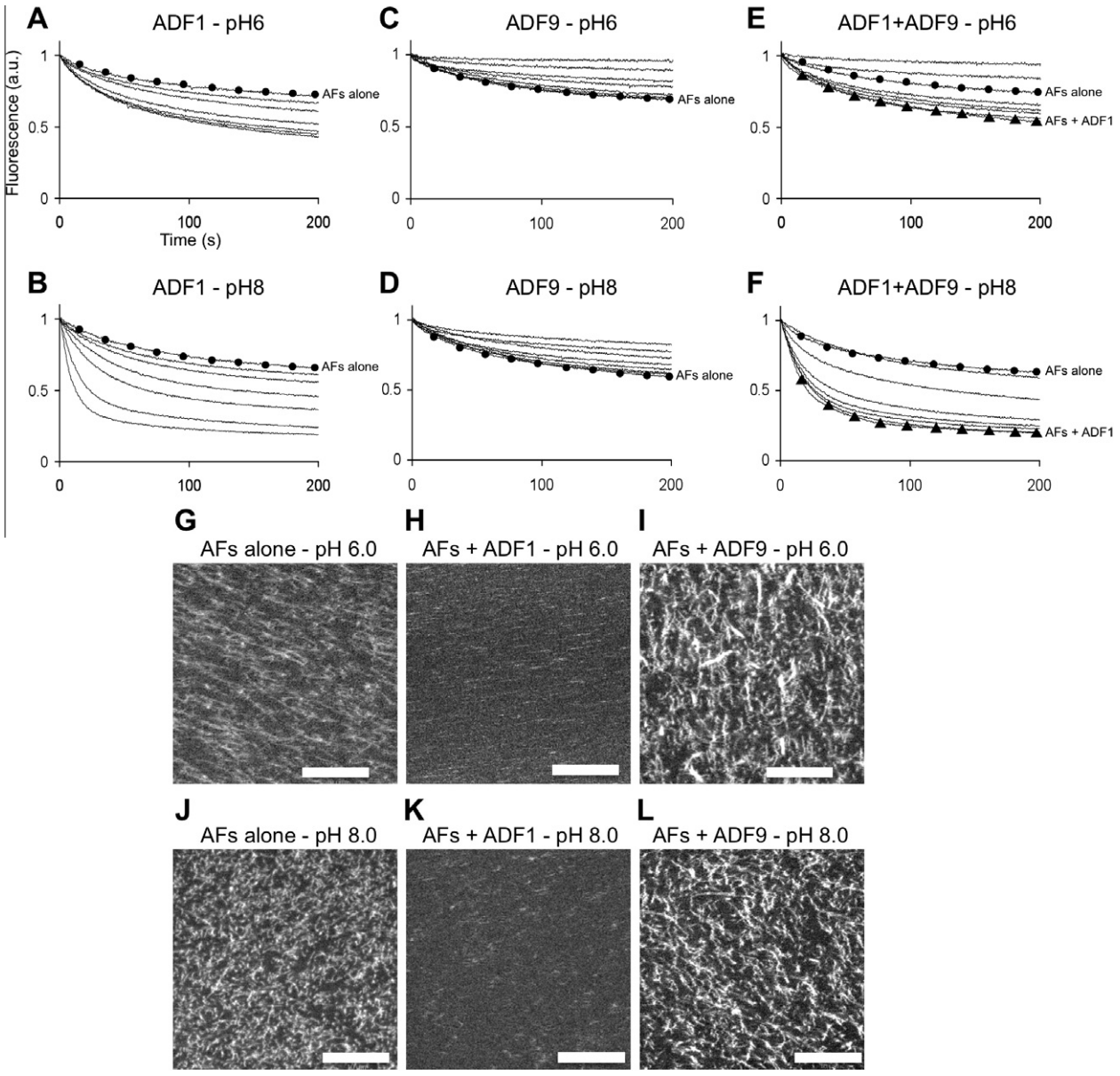

Fig. 2. ADF9 and ADF1 have opposite effects on actin dynamics. (A–D) Pyrene-labeled AFs (4 μM) were induced to depolymerize by a 10-fold dilution (400 nM actin final) in the presence of various amounts of ADF1 (8, 16, 40, 80, 160, 400 nM from top to bottom curves; A and B) or ADF9 (8, 16, 40, 80, 160, 400, 800 nM from bottom to top curves; C and D) at pH 6.0 (A and C) or pH 8.0 (B and D). Notice that ADF1 enhances and ADF9 slows down the decrease of fluorescence induced by sample dilution. (E and F) Competition experiments conducted with a fixed amount of ADF1 (160 nM, black triangles) and various amounts of ADF9 (16, 40, 80, 160, 400, 800 nM from bottom to top curves) at pH 6.0 (E) or pH 8.0 (F). Control curves obtained with AFs alone are indicated by black circles (A–F). (G–L) Direct visualization by fluorescence microscopy of Alexa-488-phalloidin stained AFs 200 s after sample dilution in the above fluorimetric assays. Conditions: 400 nM actin alone (G and J) or with 160 nM ADF1 (H and K) or ADF9 (I and L) at pH 6.0 (G–I) or pH 8.0 (J–L). Bars = 10 μm.

Together the above data suggest that, in the same range of concentrations, ADF1 and ADF9 modify actin dynamics in opposite directions and compete with each other. However, their respective levels of activity at different pH suggest that they are regulated in a coordinated manner to some extent. Indeed, ADF9 exhibits the strongest binding and stabilizing activities in acidic conditions when ADF1 depolymerizing activity is reduced, whereas it is less active in alkaline conditions when ADF1 depolymerizes AFs with the highest efficiency.

3.2. ADF9 promotes the formation of actin bundles in an autonomous manner

The atypical ability of ADF9 to inhibit actin depolymerization prompted us to investigate whether ADF9 can modify the spatial organization of AFs. Actin filaments (4 μM) were copolymerized with ADF9 (0.2–8 μM) in different pH conditions and subsequently centrifuged at low speed (12 000×*g*). At pH 6.0, the amount of pelleted actin increased proportionally to ADF9 concentration, indicating that ADF9 promoted the formation of higher-order actin structures (Fig. 3A and B, white bars). Maximum actin sedimentation (about 80% of total actin) occurred for ADF9:actin molar ratios $\geqslant$1:1 (Fig. 3B). The nature of the ADF9-induced structures was directly characterized by fluorescence light microscopy after Alexa-488-phalloidin labeling. Fig. 3C shows the typical dense network of random filaments that formed upon polymerization of 4 μM of actin. Examination of diluted samples confirmed that such a network primarily consists of unbranched AFs (Fig. 2D). In the presence of ADF9, filaments organized into long and thick actin bundles (Fig. 3E and F). In agreement with depolymerization and

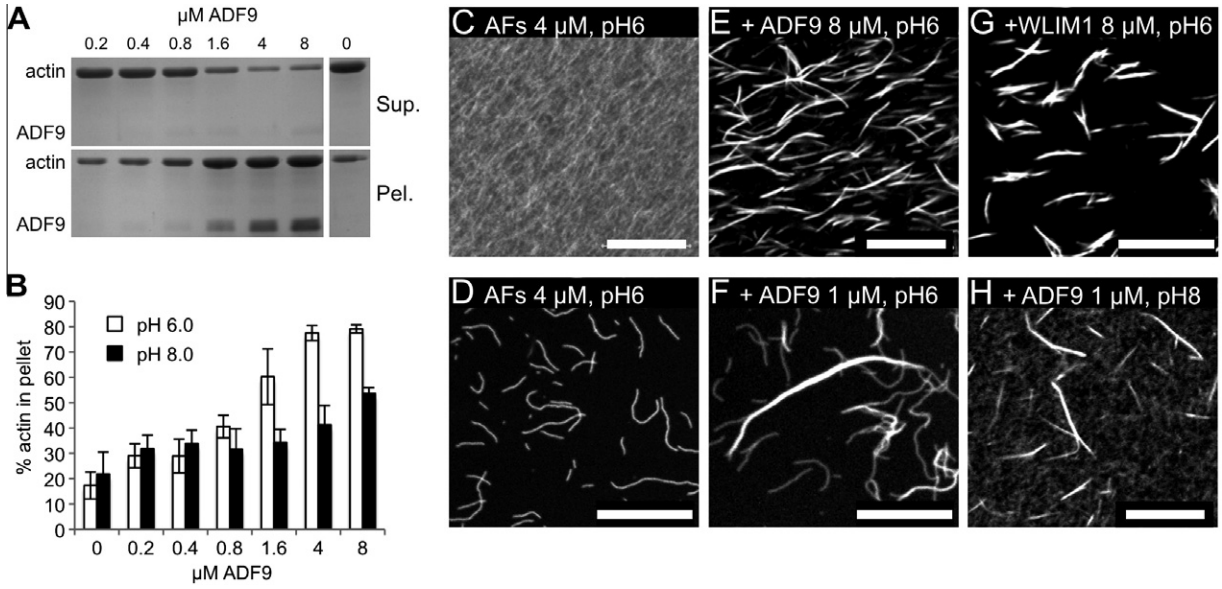

Fig. 3. ADF9 bundles actin filaments. (A) Example of a low speed cosedimentation experiment conducted at pH 6.0. AFs (4 μM) were copolymerized with various amounts of ADF9 (0.2–8 μM) and centrifuged at 12 000×*g*. The resulting supernatant (Sup.) and pellet (Pel.) fractions were analyzed by SDS–PAGE. (B) The experiment described in (A) was repeated four times at both pH 6.0 and 8.0, and the amount of actin in the supernatant and pellet fractions was quantified by densitometry. Data are presented as the percentage of total actin which sediments in each condition (white columns: pH 6.0; black columns: pH 8.0). Error bars indicate standard deviations ($n = 4$). (C–H) Direct visualization of actin bundles induced by ADF9 and WLIM1 by fluorescence microscopy after Alexa-488-phalloidin staining. (C) Control: AFs (4 μM) polymerized alone. (D) Same as (C) but the sample was diluted to 10 nM actin prior to observation in order to better visualize individual filaments. (E) Actin filaments (4 μM) copolymerized with 8 μM ADF9 (non-diluted sample). Note the absence of background fluorescence indicating that most filaments are bundled. (F) A long actin bundle formed by copolymerization of actin (4 μM) with 1 μM ADF9 (diluted to 10 nM actin prior to observation). (G) Actin filaments (4 μM) copolymerized with 8 μM of the actin bundling protein WLIM1 at pH 6.0. (H) Actin filaments (4 μM) copolymerized with 8 μM ADF9 at pH 8.0. Note the presence of significant background fluorescence (compare to E) indicating that many filaments are not bundled. Bars = 10 μm.

cosedimentation data, 1 μM ADF9 only induced partial filament bundling, whereas 8 μM ADF9 triggered a maximal effect with most AFs incorporated into bundles (Fig. 3F and E, respectively). These bundles were similar in length and shape to those induced in the same conditions by the previously characterized actin bundling protein WLIM1 (Fig. 3G; [27]). Importantly, ADF9 readily bundled pre-polymerized actin samples with an efficiency similar to the one in copolymerization experiments (data not shown). This supports that ADF9 directly crosslinks AFs and that the formation of actin monomer–ADF9 complexes is not required for the assembly of actin bundles. In contrast, no such bundles were observed in control experiments conducted with ADF1 (data not shown).

Alkaline conditions (pH 8.0) significantly reduced ADF9 bundling activity (Fig. 3B, black bars). Indeed, only 40% and 50% of total actin sedimented in the presence of 4 and 8 μM of ADF9, respectively. Accordingly, microscopical analyses revealed that actin samples that were polymerized in the presence of relatively high amounts of ADF9 contained both bright actin bundles and significant levels of background fluorescence corresponding to uncrosslinked AFs (Fig. 3H).

These data suggest that ADF9 functions as an actin bundling protein whose activity is modulated by pH conditions.

3.3. ADF9 promotes actin-bundling in vivo

In order to verify that ADF9 also promotes the formation of actin bundles in a cellular context, its coding sequence was fused to a *GFP* reporter gene and ectopically expressed in tobacco BY2 cells following biolistic transformation. The ADF9–GFP fusion protein predominantly localized to a network of thick and long cytoplasmic bundles (Fig. 4A and B). Interestingly, the thickness of the bundles decorated by ADF9–GFP increased proportionally to the amount of plasmid used for cell transformation, whereas their density decreased (compare Fig. 4A and B). This strongly supports that ADF9 promotes actin bundling in vivo. Consistent with the previously proposed role of ADF9 in the regulation of gene expression [19], significant fluorescence was also observed in the nucleus (Fig. 4A and B). Similar results were obtained when GFP was fused to the N-terminal amino acid of ADF9 (data not shown). Co-labeling experiments with rhodamine–phalloidin confirmed that ADF9–GFP interacts with the actin cytoskeleton (Fig. 4G–I). Interestingly, many ADF9–GFP expressing cells were recalcitrant to rhodamine–phalloidin staining (data not shown). Previous studies have established that ADF/cofilins and phalloidin compete with each other for actin binding (e.g. [25,28,29]). Thus, although ADF9 displays atypical bundling activity, it likely retains classical ADF/cofilin F-actin binding sites.

The extensively bundled cytoskeleton in ADF9–GFP expressing cells strikingly differed from the typical dense cortical and perinuclear arrays of rather fine filaments and bundles revealed by the talin- and fimbrin-derived actin markers (Fig. 4D and E). To rule out any possible artifact due to the presence of the GFP moiety, the effects of an untagged ADF9 version on the actin cytoskeleton organization of BY2 cells was indirectly monitored by imaging Talin-YFP in co-bombardment experiments. Similarly to the GFP-fused version, untagged ADF9 markedly modified the actin cytoskeleton organization with a significant increase in actin bundling (compare Figs. 4E and 3F).

In contrast to ADF9–GFP, ADF1–GFP decorated a network of randomly distributed short, severed-like, bundles (Fig. 4C). The latter were usually not stable over time and most of them disappeared 24 h after cell transfection (data not shown). These observations are consistent with previous studies conducted in transgenic plants showing that ADF1 promotes actin cytoskeleton depolymerization [18] and further support that ADF1 severs AFs and bundles in vivo.

Thus, both biochemical data and live cell experiments support that ADF9 functions as an actin bundling protein and lacks typical

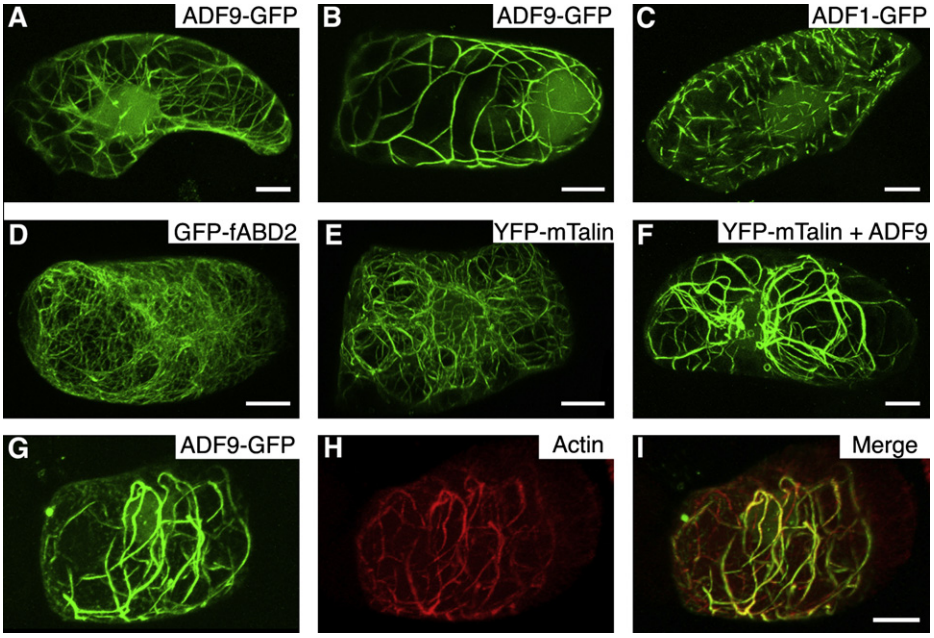

Fig. 4. ADF9 promotes actin bundling in live cells. (A–C) Typical subcellular localization of ADF9–GFP (A and B) and ADF1–GFP (C) in tobacco BY2 cells. (D and E) Typical actin cytoskeleton organization in BY2 cells as visualized by fimbrin- (D) and talin- (E) derived actin markers. (F) Modification of the actin cytoskeleton organization triggered by untagged ADF9 as visualized by the YFP-mTalin marker. Notice the significant increase in actin bundling (compare to E). (G–I) Colocalization of ADF9–GFP and the actin cytoskeleton. A tobacco BY2 cell expressing ADF9–GFP (G) was labeled with rhodamine-phalloidin (H). The extensive yellow signal in the merged image (I) indicates that ADF9–GFP interacts with the actin cytoskeleton. The confocal stack images shown in (B–G) were obtained after biolistic transfection of BY2 cells using gold particles coated with 1 μg of appropriate plasmid(s). The confocal stack image shown in (A) was obtained using only 0.02 μg of the ADF9–GFP encoding plasmid. Bars = 10 μm.

ADF/cofilin actin depolymerizing and/or severing activities. Although elevated levels of ADF/cofilins have been previously reported to increase actin-bundling in different cell types including *Dictyostelium*, mammalian and plant cells [30–33], this was not correlated with an intrinsic capacity of ADF/cofilin to crosslink AFs. As previously stated, ADF1 and ADF9 are relatively distant members of the *Arabidopsis* ADF protein family with 53% identity and 78% similarity (Fig. 5A). However, very similar secondary and tertiary structures are expected from protein homology modeling (Fig. 5A and B, respectively). Interestingly, substantial movement is predicted in the F loop and adjacent C-terminal helix of the F-actin biding site (Fig. 5B). Although this remains speculative, this might confer ADF1 and ADF9 different affinities for AFs.

A variety of stress conditions and pathologies induce the formation of rod-shaped actin bundles (actin rods) in animal cells (e.g. [29,34–37]). Actin rod-like structures have also been observed to form in the nucleus of plant cells treated with cytochalasin D [28]. Noticeably, many types of actin rods are heavily decorated by ADF/cofilins, suggesting central roles of the latter in their formation. A recent study has provided evidence that AFs and ADF/cofilins are the major components (in a 1:1 ratio) of actin rods induced by ATP depletion, and that equimolar amounts of purified

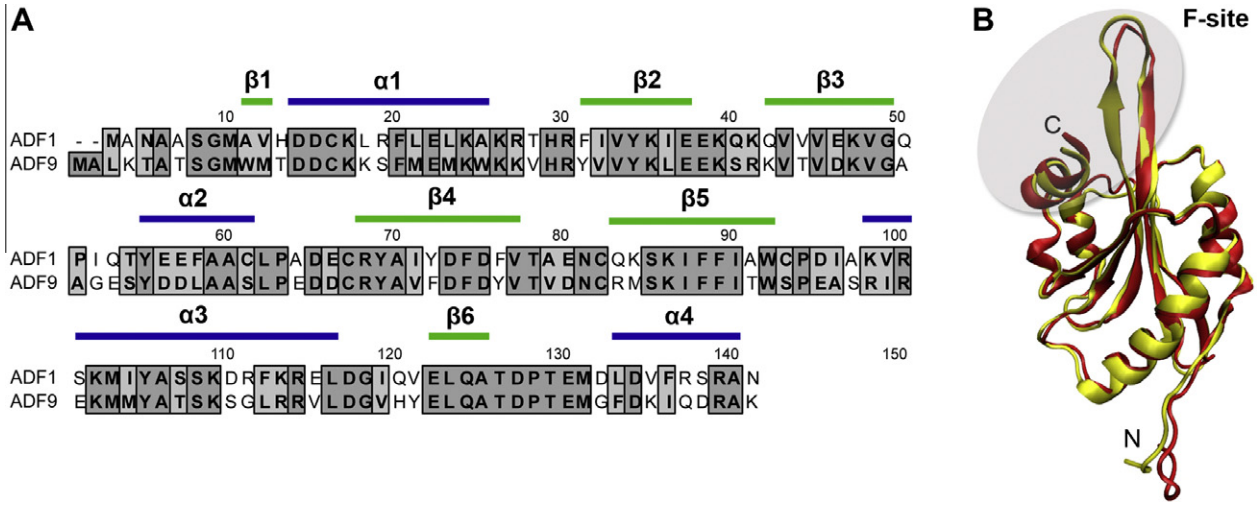

Fig. 5. Structural comparison of *Arabidopsis* ADF1 and ADF9. (A) Amino acid sequence alignment of *Arabidopsis* ADF1 and ADF9. Shaded boxes and bold letters indicate amino acid identities and similarities in dark and light gray, respectively. The secondary structural elements are indicated above the alignment in blue for α-helices and green for β-sheets. (B) Superimposition of the crystal structure of ADF1 [17] (red) and predicted structure of ADF9 (yellow). The shaded region (F-site) indicates the F-actin binding site which includes the F-loop and the adjacent C-terminal helix.

actin and cofilin are sufficient to generate rod-like structures in vitro [38]. Although ADF/cofilin-actin rods and ADF9-induced actin bundles are unlikely equivalent structures, their formation might involve a similar mechanism. Pfannstiel et al. (2001) provided evidence that human cofilin possesses an intrinsic tendency for self-association, although the equilibrium in a cofilin solution is usually toward the monomer [39]. They showed that chemically stabilized cofilin dimers and oligomers lack depolymerizing activity but exhibit actin bundling activity instead. Future work should establish whether ADF9 has a particularly high capacity to dimerize or oligomerize, which could account for its atypical activity.

Acknowledgements

We thank B. Kost (Uppsala Genetic Center, SLU, Sweden) for providing the YFP-Talin construct and D. McCurdy (University of Newcastle, NSW, Australia) for the GFP-fABD2 construct. This work was supported by the Ministry of Culture, Higher Education, and Research and by the National Research Fund (Luxembourg).

References

[1] Bernstein, B.W. and Bamburg, J.R. (2010) ADF/cofilin: a functional node in cell biology. Trends Cell Biol. 20, 187–195.
[2] Van Troys, M., Huyck, L., Leyman, S., Dhaese, S., Vandekerkhove, J. and Ampe, C. (2008) Ins and outs of ADF/cofilin activity and regulation. Eur. J. Cell Biol. 87, 649–667.
[3] Andrianantoandro, E. and Pollard, T.D. (2006) Mechanism of actin filament turnover by severing and nucleation at different concentrations of ADF/cofilin. Mol. Cell 24, 13–23.
[4] Blanchoin, L. and Pollard, T.D. (1999) Mechanism of interaction of *Acanthamoeba* actophorin (ADF/cofilin) with actin filaments. J. Biol. Chem. 274, 15538–15546.
[5] Carlier, M.F. et al. (1997) Actin depolymerizing factor (ADF/cofilin) enhances the rate of filament turnover: implication in actin-based motility. J. Cell Biol. 136, 1307–1322.
[6] Maciver, S.K. and Hussey, P.J. (2002) The ADF/cofilin family: actin-remodeling proteins. Genome Biol. 3. reviews3007.
[7] McGough, A., Pope, B., Chiu, W. and Weeds, A. (1997) Cofilin changes the twist of F-actin: implications for actin filament dynamics and cellular function. J. Cell Biol. 138, 771–781.
[8] Pope, B.J., Gonsior, S.M., Yeoh, S., McGough, A. and Weeds, A.G. (2000) Uncoupling actin filament fragmentation by cofilin from increased subunit turnover. J. Mol. Biol. 298, 649–661.
[9] Ressad, F., Didry, D., Xia, G.X., Hong, Y., Chua, N.H., Pantaloni, D. and Carlier, M.F. (1998) Kinetic analysis of the interaction of actin-depolymerizing factor (ADF)/cofilin with G- and F-actins. Comparison of plant and human ADFs and effect of phosphorylation. J. Biol. Chem. 273, 20894–20902.
[10] Chen, H., Bernstein, B.W., Sneider, J.M., Boyle, J.A., Minamide, L.S. and Bamburg, J.R. (2004) In vitro activity differences between proteins of the ADF/cofilin family define two distinct subgroups. Biochemistry 43, 7127–7142.
[11] Yeoh, S., Pope, B., Mannherz, H.G. and Weeds, A. (2002) Determining the differences in actin binding by human ADF and cofilin. J. Mol. Biol. 315, 911–925.
[12] Blanchoin, L., Pollard, T.D. and Mullins, R.D. (2000) Interactions of ADF/cofilin, Arp2/3 complex, capping protein and profilin in remodeling of branched actin filament networks. Curr. Biol. 10, 1273–1282.
[13] Chan, C., Beltzner, C.C. and Pollard, T.D. (2009) Cofilin dissociates Arp2/3 complex and branches from actin filaments. Curr. Biol. 19, 537–545.
[14] Maciver, S.K. (1998) How ADF/cofilin depolymerizes actin filaments. Curr. Opin. Cell Biol. 10, 140–144.
[15] Ruzicka, D.R., Kandasamy, M.K., McKinney, E.C., Burgos-Rivera, B. and Meagher, R.B. (2007) The ancient subclasses of *Arabidopsis* actin depolymerizing factor genes exhibit novel and differential expression. Plant J. 52, 460–472.
[16] Kandasamy, M.K., Burgos-Rivera, B., McKinney, E.C., Ruzicka, D.R. and Meagher, R.B. (2007) Class-specific interaction of profilin and ADF isovariants with actin in the regulation of plant development. Plant Cell 19, 3111–3126.
[17] Bowman, G.D., Nodelman, I.M., Hong, Y., Chua, N.H., Lindberg, U. and Schutt, C.E. (2000) A comparative structural analysis of the ADF/cofilin family. Proteins 41, 374–384.
[18] Dong, C.H., Xia, G.X., Hong, Y., Ramachandran, S., Kost, B. and Chua, N.H. (2001) ADF proteins are involved in the control of flowering and regulate F-actin organization, cell expansion, and organ growth in *Arabidopsis*. Plant Cell 13, 1333–1346.
[19] Burgos-Rivera, B., Ruzicka, D.R., Deal, R.B., McKinney, E.C., King-Reid, L. and Meagher, R.B. (2008) Actin depolymerizing factor 9 controls development and gene expression in *Arabidopsis*. Plant Mol. Biol. 68, 619–632.
[20] Sali, A. and Blundell, T.L. (1993) Comparative protein modelling by satisfaction of spatial restraints. J. Mol. Biol. 234, 779–815.
[21] Brooks, B.R., Bruccoleri, R.E., Olafson, B.D., States, D.J., Swaminathan, S. and Karplus, M. (1983) CHARMM: a program for macromolecular energy, minimization, and dynamics calculations. J. Comput. Chem. 4, 187–217.
[22] Allwood, E.G., Anthony, R.G., Smertenko, A.P., Reichelt, S., Drobak, B.K., Doonan, J.H., Weeds, A.G. and Hussey, P.J. (2002) Regulation of the pollen-specific actin-depolymerizing factor LlADF1. Plant Cell 14, 2915–2927.
[23] Gungabissoon, R.A., Jiang, C.J., Drobak, B.K., Maciver, S.K. and Hussey, P.J. (1998) Interaction of maize actin-depolymerising factor with actin and phosphoinositides and its inhibition of plant phospholipase C. Plant J. 16, 689–696.
[24] Hawkins, M., Pope, B., Maciver, S.K. and Weeds, A.G. (1993) Human actin depolymerizing factor mediates a pH-sensitive destruction of actin filaments. Biochemistry 32, 9985–9993.
[25] Hayden, S.M., Miller, P.S., Brauweiler, A. and Bamburg, J.R. (1993) Analysis of the interactions of actin depolymerizing factor with G- and F-actin. Biochemistry 32, 9994–10004.
[26] Yonezawa, N., Nishida, E. and Sakai, H. (1985) PH control of actin polymerization by cofilin. J. Biol. Chem. 260, 14410–14412.
[27] Papuga, J., Hoffmann, C., Dieterle, M., Moes, D., Moreau, F., Tholl, S., Steinmetz, A. and Thomas, C. (2010) Arabidopsis LIM proteins: a family of actin bundlers with distinct expression patterns and modes of regulation. Plant Cell 22, 3034–3052.
[28] Jiang, C.J., Weeds, A.G. and Hussey, P.J. (1997) The maize actin-depolymerizing factor, ZmADF3, redistributes to the growing tip of elongating root hairs and can be induced to translocate into the nucleus with actin. Plant J. 12, 1035–1043.
[29] Nishida, E., Iida, K., Yonezawa, N., Koyasu, S., Yahara, I. and Sakai, H. (1987) Cofilin is a component of intranuclear and cytoplasmic actin rods induced in cultured cells. Proc. Natl. Acad. Sci. USA 84, 5262–5266.
[30] Aizawa, H., Fukui, Y. and Yahara, I. (1997) Live dynamics of *Dictyostelium* cofilin suggests a role in remodeling actin latticework into bundles. J. Cell Sci. 110 (Pt 19), 2333–2344.
[31] Aizawa, H., Sutoh, K. and Yahara, I. (1996) Overexpression of cofilin stimulates bundling of actin filaments, membrane ruffling, and cell movement in *Dictyostelium*. J. Cell Biol. 132, 335–344.
[32] Hussey, P.J., Yuan, M., Calder, G., Khan, S. and Lloyd, C.W. (1998) Microinjection of pollen-specific actin-depolymerizing factor, ZmADF1, reorients F-actin strands in *Tradescantia* stamen hair cells. Plant J. 14, 353–357.
[33] Moriyama, K., Iida, K. and Yahara, I. (1996) Phosphorylation of Ser-3 of cofilin regulates its essential function on actin. Genes Cells 1, 73–86.
[34] Ashworth, S.L., Southgate, E.L., Sandoval, R.M., Meberg, P.J., Bamburg, J.R. and Molitoris, B.A. (2003) ADF/cofilin mediates actin cytoskeletal alterations in LLC-PK cells during ATP depletion. Am. J. Physiol. Renal Physiol. 284, F852–F862.
[35] Bamburg, J.R. et al. (2010) ADF/cofilin-actin rods in neurodegenerative diseases. Curr. Alzheimer Res. 7, 241–250.
[36] Minamide, L.S., Striegl, A.M., Boyle, J.A., Meberg, P.J. and Bamburg, J.R. (2000) Neurodegenerative stimuli induce persistent ADF/cofilin-actin rods that disrupt distal neurite function. Nat. Cell Biol. 2, 628–636.
[37] Ono, S., Abe, H., Nagaoka, R. and Obinata, T. (1993) Colocalization of ADF and cofilin in intranuclear actin rods of cultured muscle cells. J. Muscle Res. Cell Motil. 14, 195–204.
[38] Minamide, L.S. et al. (2010) Isolation and characterization of cytoplasmic cofilin-actin rods. J. Biol. Chem. 285, 5450–5460.
[39] Pfannstiel, J., Cyrklaff, M., Habermann, A., Stoeva, S., Griffiths, G., Shoeman, R. and Faulstich, H. (2001) Human cofilin forms oligomers exhibiting actin bundling activity. J. Biol. Chem. 276, 49476–49484.